NOLTA, IEICE

Paper

Performance comparison of stochastic resonance receiver with Schmitt trigger, comparator, and three-level device for subthreshold signal reception

Hiroya Tanaka [1 a)], *Takaya Yamazato* [1], *Yukihiro Tadokoro* [2], *and Shintaro Arai* [3]

[1] *Nagoya University, Furo-cho, Chikusa-ku, Nagoya 464-8603, Japan*

[2] *Toyota Central R&D Laboratories, Inc., Aichi 480-1192, Japan*

[3] *Okayama University of Science, 1-1 Ridai-cho, Kita-ku, Okayama 700-0005, Japan*

[a)] *tanaka@katayama.nuee.nagoya-u.ac.jp*

Received September 17, 2015; Revised February 3, 2016; Published July 1, 2016

Abstract: This paper discusses the stochastic resonance (SR) effect in a binary communication system for subthreshold signal reception. We focus on the problem of no communication when received signal strength is below receiver sensitivity. Subthreshold signal reception requires a device that exhibits SR, such as a Schmitt trigger or a comparator. Previously, we proposed an alternative three-level device and demonstrated its high performance for subthreshold signal reception in an SR receiver. In the present study, we show that our proposed three-level device outperforms the three devices and discuss reasons for this superior performance. Contributions of our present paper are twofold: first, we analytically derive bit error rate (BER) performances of SR receivers installed with a Schmitt trigger and a comparator; second, we compare performances of the Schmitt trigger, comparator, and three-level device.

Key Words: stochastic resonance, intentional noise, non-dynamical, dynamical, subthreshold, Schmitt trigger, comparator, three-level device, bit error rate

1. Introduction

Stochastic resonance (SR) is a phenomenon by which a noise enhances a weak signal below a receiver's sensitivity [1–5]. Despite the attractiveness of this phenomenon, the SR effect in communication systems has been little investigated [6–8]. Overcoming receiver sensitivity, equivalently, receiving subthreshold communication signals, presents special challenges in wireless communication systems [9–11]. If we realize subthreshold wireless communication systems, we can simultaneously reduce transmission power and interference among users. Such low-power wireless systems would

Nonlinear Theory and Its Applications, IEICE, vol. 7, no. 3, pp. 407–418 DOI: 10.1587/nolta.7.407

provide energy-efficient green wireless communications and solve wireless spectrum shortage.

This paper discusses the SR effect in a binary communication system for subthreshold signal reception. We focus on the problem in which communication cannot be established when received signal strength falls below receiver sensitivity. For subthreshold signal reception, we require a device that exhibits SR, such as a Schmitt trigger or a comparator. Previously, we proposed an alternative three-level device and demonstrated its relatively good performance for subthreshold signal reception in an SR receiver [10].

A Schmitt trigger is a well-known SR-exhibiting device [12–14]. Because the trigger's output is fixed to one of two voltages, its dynamics are modeled as two-state systems. Furthermore, the trigger is hysteretic within the range of inputs for which a circuit is bistable. A famous study by McNamara and Wiesenfeld demonstrates the practicality of a Schmitt trigger in SR systems [12]. Following this pioneering work, Melnikov proved that an ideal Schmitt trigger is the simplest two-state system that realizes SR [13]. As a dynamic device (possessing a memory effect), a Schmitt trigger should outperform a non-dynamical device (which lacks a memory effect). In general, because of a memory effect, dynamical systems yield higher SNR than non-dynamical system [14].

Comparators belong to the class of non-dynamical SR systems with a threshold-triggered device [12]. However, a comparator is a poor performer in subthreshold signal reception because a single threshold determines whether a signal is above the device's sensitivity. This threshold can be set positive or negative without affecting performance, but in either case, signals of opposite polarity are lost.

Contrary to popular opinion that dynamical SR systems perform better than non-dynamical systems, we have demonstrated strong subthreshold signal reception by an SR receiver installed with our three-level non-dynamical device [10]. The desirable performance of the three-level device can be explained by scrutinizing states of a subthreshold signal.

A subthreshold signal is defined as a signal below a receiver's sensitivity. Let the signal threshold be η, and suppose that a bipolar non-return-to-zero pulse is a subthreshold baseband signal that is input to an SR receiver. Then, a signal plus noise is observable by the receiver only when the signal strength exceeds $+\eta$ or $-\eta$. When the signal is below the receiver's sensitivity ($\pm\eta$), no signal is observed. Thus, a subthreshold signal is modeled as a signal with positive, negative, and zero states. Because the three-level device well corresponds to the subthreshold signal model (three-state signal), the performance of the device may exceed that of Schmitt trigger and comparator. Indeed, as shown later in this paper, the three-level device delivers the best performance among the three devices.

The present study aims to understand the superior performance of the three-level device in receiving subthreshold communication signals. Three SR devices are considered: Schmitt trigger, comparator, and three-level device. The Schmitt trigger is a dynamical device with a memory effect, whereas the comparator and three-level device are non-dynamical devices and are distinguished chiefly by their number of thresholds. The comparator has a single threshold, and the three-level device has two thresholds. To compare performances of these systems, we analytically derive the bit error rate (BER) of SR systems installed with the comparator and the Schmitt trigger and adopt the BER of the three-level device reported in [10].

Contributions of our present study are twofold: first, we analytically derive BER performances of Schmitt trigger- and comparator-based SR receivers. Because outputs of these devices are stochastic, they involve occurrence probabilities. Using these probabilities, we derive the exact BER performances and confirm their consistency with the simulation results. Second, we compare performances of Schmitt trigger, comparator, and three-level device. We discuss in detail the superior performance of the three-level device in receiving subthreshold communication signals. We further note that comparator better detects subthreshold signals than the Schmitt trigger. This result is unexpected but is traceable to the memory effect of the Schmitt Trigger, which degrades the performance of subthreshold signal reception. In numerical evaluations, the three-level device exhibits the best performance among the three devices and is strongly compatible with binary communication systems.

The remainder of this paper is organized as follows. Sections 2 and 3 present the system model and BER performance analysis, respectively, of SR receivers with the Schmitt trigger and comparator. In Section 4, BER performances and their comparisons are numerically evaluated. Conclusions are

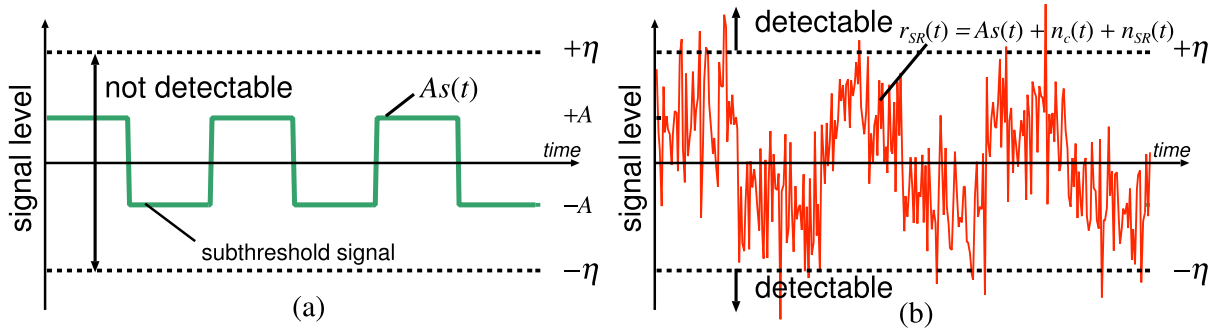

Fig. 1. Example of the subthreshold signal (a) and the subthreshold signal plus channel noise and intentional noise (b).

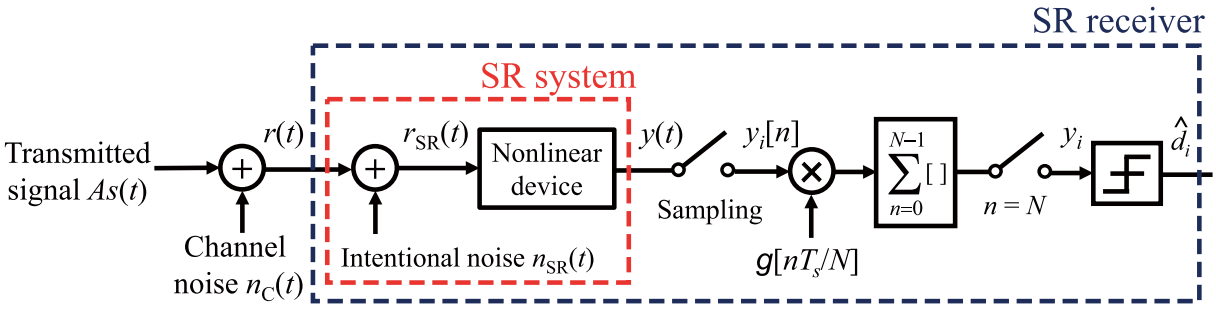

Fig. 2. System model of SR receiver.

presented in Section 5.

2. System model

In this study, a received signal level is assumed to be below receiver sensitivity. Denoting the received signal level by A and the receiver sensitivity by η, we observe that $|A| < \eta$ (see Fig. 1(a)). As shown in Fig. 1(a), such subthreshold signals cannot be detected by a conventional receiver. Furthermore, when a noise is added to the signal (Fig. 1(b)), the combined signal is observable by the receiver only when its strength exceeds $+\eta$ or $-\eta$. When the signal is below the receiver's sensitivity ($\pm\eta$), no signal is observed. Thus, a subthreshold signal is modeled as a signal with three states: positive ($+\eta$), negative ($-\eta$) and zero. As discussed later (see 4.2), the three-level device well corresponds to the subthreshold signal model (with three-state signals) and yields the best performance among the tested devices.

Figure 2 shows the system model of the SR receiver. The SR system receives a desired signal $s(t)$ and channel noise $n_c(t)$. The desired signal $s(t)$ is expressed as follows:

$$s(t) = \sum_i d_i g(t - iT_s). \tag{1}$$

Here d_i is the binary data sequence $\{\pm 1\}$ of the ith symbol, T_s is the symbol duration, and $g(t)$ is a rectangular pulse such that $g(t) = +1$ in $0 \le t < T_s/2$ and $g(t) = -1$ in $T_s/2 \le t < T_s$. This pulse signal $s(t)$, which is known as the Manchester code, is shown in the symbol duration in Fig. 3. Throughout the symbol duration, positive and negative signals have the same interval. This contributes to the decision rule. The data of $d_i = +1$ and $d_i = -1$ occur randomly.

At the receiver, the signal of level A is added to the channel noise $n_c(t)$. The received signal is expressed as follows.

$$r(t) = As(t) + n_c(t). \tag{2}$$

The channel noise $n_c(t)$ is a zero-mean white Gaussian noise with variance σ_c^2.

The channel noise is dominated by a thermal noise in the receiver; thus, its power spectral density (PSD) is assumed to be uniform. The PSD is given by $N_0 = k_B T_0$, where k_B is the Boltzmann constant

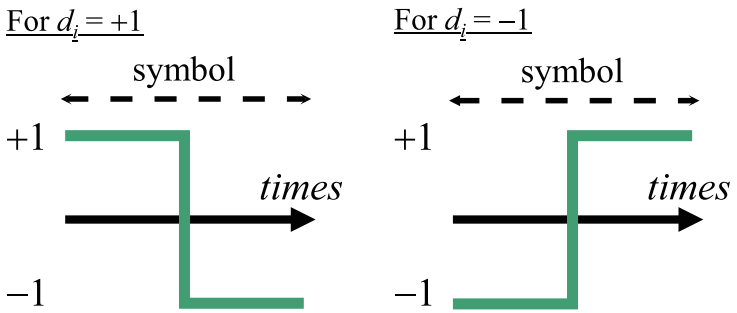

Fig. 3. Manchester code $s(t)$ in the symbol duration for $d_i = +1$ (left) and $d_i = -1$ (right).

and T_0 is the noise temperature. Setting $T_0 = 300$ K, the noise PSD is computed as $N_0 \simeq 4.1 \times 10^{-21}$ W/Hz.

Unfortunately, the channel noise is always added to the received signal and is inseparable from a signal component. Different from a conventional receiver, the SR receiver adds an intentional noise at the receiver front end and can thus detect subthreshold signals. Once a signal has been detected by the SR system, it can be managed by conventional receivers. Figure 1(b) illustrates a simple SR effect, i.e., the detection of a subthreshold signal with an additional intentional noise. The depicted signal is obtained by adding both channel and intentional noises to the subthreshold signal shown in Fig. 1(a). The intentional noise $n_{SR}(t)$, assumed as the zero-mean white Gaussian noise with variance σ^2_{SR}, should be tuned to optimize SR receiver performance.

Reception sensitivity can be modeled as the threshold of simple nonlinear devices exhibiting the SR effect. The received signal, composed of $As(t)$, $n_c(t)$, and $n_{SR}(t)$, is fed into the nonlinear device. In this study, comparator and Schmitt trigger are adopted as the non-dynamical and dynamical devices, respectively. In 4.2, performances of both devices are compared with that of the three-level device [10].

Input-output characteristics of the comparator and Schmitt trigger are shown in Fig. 4. Note that the comparator has two outputs and one threshold. Although the Schmitt trigger exhibits hysteresis from the memory effect, the comparator outputs depend on current input. Provided that the subthreshold signal plus noise exceeds the threshold, the subthreshold signal is detectable when the noise is optimally tuned. This phenomenon is known as SR.

The output of the comparator in response to an input signal $r_{SR}(t)$ is given by

$$y(t) = \begin{cases} +V & (r_{\mathrm{SR}}(t) > \eta) \\ -V & otherwise \end{cases}. \tag{3}$$

In the Schmitt trigger, the threshold depends current state as follows:

$$V_{th} = \begin{cases} -\eta & if \quad y(t) = +V \\ +\eta & if \quad y(t) = -V \end{cases}. \tag{4}$$

A Schmitt trigger fed with an input signal $r_{SR}(t)$ yields the output as follows:

$$y(t) = \begin{cases} -V & if \quad r_{SR}(t) < V_{th} \\ +V & if \quad r_{SR}(t) > V_{th} \end{cases}. \tag{5}$$

The threshold η of the Schmitt trigger or comparator is assumed equivalent to the reception sensitivity of a conventional receiver.

These outputs of non-linear devices are sampled N times during the symbol duration and are multiplied by $g(t)$ for detection. Denoting a sample of the device output as $y_i[n]$, we express the decision variable y_i as

$$y_i = \sum_{n=0}^{N-1} y_i[n] g[nT_s/N]. \tag{6}$$

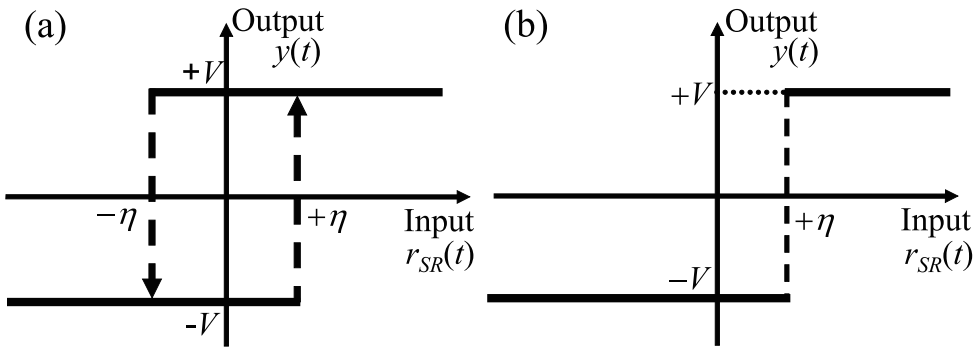

Fig. 4. Input-Output characteristics of a Schmitt trigger (a) and a Comparator (b).

The data are restored in the detector using the decision variable with a decision threshold. Data restoration depends on whether the output is positive or negative as shown below:

$$\hat{d}_i = \begin{cases} +1 & (y_i > 0) \\ -1 & otherwise \end{cases}. \tag{7}$$

That is, the detector makes the major decision. The BER performance improves with increasing N. In our system, high sampling rate will enhance the subthreshold signal. Thus, our system is applicable to small-bandwidth scenarios.

Note that decision making is based on characteristics of the device and the desired signal. Because comparator thresholds are asymmetric (see Fig. 4(b)). $P[y(t) = +V]$ and $P[y(t) = -V]$ are asymmetric between the signal levels $+A$ and $-A$. To avoid this asymmetry, we specify that signals in the data $d_i = \pm 1$ become positive and negative over identical intervals during the symbol duration.

3. BER analysis method for the SR system

In this section, we analytically evaluate the BER performance of comparator- and Schmitt trigger-based SR systems. These devices output $+V$ or $-V$ with probabilities depending on the input $r_{SR(t)}$. We derive these probabilities and thereby calculate the BER.

3.1 Comparator

In response to a Gaussian input $r_{SR}(t)$, with mean $As(t)$ and variance $\sigma_c^2 + \sigma_{SR}^2$, the comparator stochastically outputs the value $-V$ or $+V$. The probability of a $+V$ output is straightforwardly derived as

$$P[y(t) = +V] = \frac{1}{2}\mathrm{erfc}\left(\frac{\eta - As(t)}{\sqrt{2(\sigma_{\mathrm{c}}^2 + \sigma_{\mathrm{SR}}^2)}}\right). \tag{8}$$

In Eq. (8), $\mathrm{erfc}(u) = \frac{2}{\sqrt{\pi}} \int_u^{+\infty} \exp(-t^2)dt$ is the complementary error function. The probability of a $-V$ output is then derived as

$$\begin{aligned} P[y(t) = -V] &= 1 - P[y(t) = +V]. \\ &= 1 - \frac{1}{2}\mathrm{erfc}\left(\frac{\eta - As(t)}{\sqrt{2(\sigma_{\mathrm{c}}^2 + \sigma_{\mathrm{SR}}^2)}}\right). \end{aligned} \tag{9}$$

The data restoration decision depends on the output of the SR system (see Eq. (7)). The data are restored as $+1$ if $+V$ is sampled at least $N/2$ times; otherwise, they are restored as -1. Note that because input signals are assumed as the Manchester code (Fig. 3), the sample number is $N/2$ whenever $+V$ or $-V$ is sampled. The BER is then derived as follows:

$$
\begin{aligned}
\mathrm{BER} &= P[\hat{d}_i = +1|d_i = -1]P[d_i = -1] + P[\hat{d}_i = -1|d_i = +1]P[d_i = +1]. \\
&= \frac{1}{2}P[y_i > 0|d_i = -1] + \frac{1}{2}P[y_i \le 0|d_i = +1]. \\
&= \frac{1}{2}P\big[\sum_{n=0}^{N-1} y_i[n]g[nT_s/N] > 0|d_i = -1\big] + \frac{1}{2}P\big[\sum_{n=0}^{N-1} y_i[n]g[nT_s/N] \le 0|d_i = +1\big]. \qquad (10)
\end{aligned}
$$

If $d_i = -1$, an error occurs when the number of samples $y_i[n] = -V$ in $0 \le n < N/2$ or when $y_i[n] = +V$ in $N/2 \le n < N$ is less than $N/2$. This error arises because $g(t) = -1$ in $0 \le t < T_s/2$ and $g(t) = +1$ in $T_s/2 \le t < T_s$. After $N/2$ trials, occurrence probabilities of these events follow a binomial distribution. Denoting the number of samples $y_i[n] = -V$ in $0 \le n < N/2$ and $y_i[n] = +V$ in $N/2 \le n < N$ as x and y, respectively, and assuming binomial distributions, the first term in Eq. (10) becomes

$$
\begin{aligned}
&P\big[\sum_{n=0}^{N-1} y_i[n]g[nT_s/N] > 0|d_i = -1\big]. \\
&= \sum_{\substack{0\le x+y<N/2 \\ x\le N/2, y\le N/2}} \binom{N/2}{x} P[y(t) = -V|d_i = -1]^x P[y(t) = +V|d_i = -1]^{N/2-x} \\
&\qquad \times \binom{N/2}{y} P[y(t) = +V|d_i = -1]^y P[y(t) = -V|d_i = -1]^{N/2-y}. \\
&= \sum_{\substack{0\le x+y<N/2 \\ x\le N/2, y\le N/2}} \binom{N/2}{x} \Big\{1 - \frac{1}{2}\mathrm{erfc}\Big(\frac{\eta + A}{\sqrt{2(\sigma_c^2 + \sigma_{SR}^2)}}\Big)\Big\}^x \Big\{\frac{1}{2}\mathrm{erfc}\Big(\frac{\eta + A}{\sqrt{2(\sigma_c^2 + \sigma_{SR}^2)}}\Big)\Big\}^{N/2-x} \\
&\qquad \times \binom{N/2}{y} \Big\{\frac{1}{2}\mathrm{erfc}\Big(\frac{\eta - A}{\sqrt{2(\sigma_c^2 + \sigma_{SR}^2)}}\Big)\Big\}^y \Big\{1 - \frac{1}{2}\mathrm{erfc}\Big(\frac{\eta - A}{\sqrt{2(\sigma_c^2 + \sigma_{SR}^2)}}\Big)\Big\}^{N/2-y}. \qquad (11)
\end{aligned}
$$

The error probability for $d_i = +1$ is derived in the same manner. In the case that N is even, these error probability of $d_i = -1$ or $d_i = +1$ are identical. In this present study, we set N is even. For even N, we derive the BER for the comparator-based SR as follows:

$$
\begin{aligned}
&\mathrm{BER} \\
&= \sum_{\substack{0\le x+y<N/2 \\ x\le N/2, y\le N/2}} \binom{N/2}{x} \Big\{1 - \frac{1}{2}\mathrm{erfc}\Big(\frac{\eta + A}{\sqrt{2(\sigma_c^2 + \sigma_{SR}^2)}}\Big)\Big\}^x \Big\{\frac{1}{2}\mathrm{erfc}\Big(\frac{\eta + A}{\sqrt{2(\sigma_c^2 + \sigma_{SR}^2)}}\Big)\Big\}^{N/2-x} \\
&\qquad \times \binom{N/2}{y} \Big\{\frac{1}{2}\mathrm{erfc}\Big(\frac{\eta - A}{\sqrt{2(\sigma_c^2 + \sigma_{SR}^2)}}\Big)\Big\}^y \Big\{1 - \frac{1}{2}\mathrm{erfc}\Big(\frac{\eta - A}{\sqrt{2(\sigma_c^2 + \sigma_{SR}^2)}}\Big)\Big\}^{N/2-y} \qquad (12)
\end{aligned}
$$

If N is odd, we can derive it in the same manner. Note that N being even or odd does not affect the BER performance.

3.2 Schmitt trigger

To analyze the device using the Schmitt trigger, we adopt the Markov model shown in Fig. 5. This model has two, indicated "$-V$" and "$+V$". In the "$-V$" state, the Schmitt trigger outputs $-V$; in the "$+V$" state, it outputs $+V$. In the present study, we initialize this model to the "$+V$" state. The probability of a transition from state i to j, where $i, j \in \{-V, +V\}$, is denoted by $P_{i\to j}$. Transition probabilities and outputs are illustrated in Fig. 5. Transition probabilities are as follows:

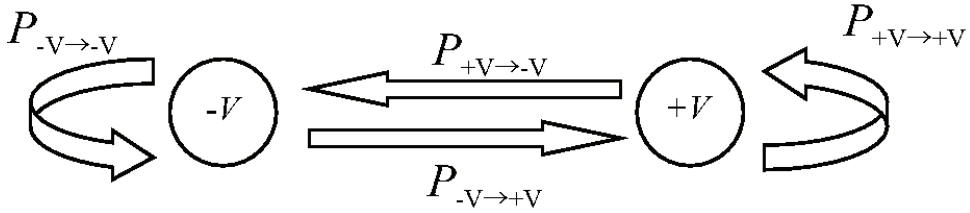

Fig. 5. Analysis model for the Schmitt trigger.

$$P_{-V\to-V} = 1 - \frac{1}{2}\mathrm{erfc}\left(\frac{\eta - As(t)}{\sqrt{2(\sigma_c^2 + \sigma_{SR}^2)}}\right). \tag{13}$$

$$P_{-V\to+V} = \frac{1}{2}\mathrm{erfc}\left(\frac{\eta - As(t)}{\sqrt{2(\sigma_c^2 + \sigma_{SR}^2)}}\right). \tag{14}$$

$$P_{+V\to-V} = \frac{1}{2}\mathrm{erfc}\left(\frac{\eta + As(t)}{\sqrt{2(\sigma_c^2 + \sigma_{SR}^2)}}\right). \tag{15}$$

$$P_{+V\to+V} = 1 - \frac{1}{2}\mathrm{erfc}\left(\frac{\eta + As(t)}{\sqrt{2(\sigma_c^2 + \sigma_{SR}^2)}}\right). \tag{16}$$

As shown in Eq. (10), the BER depends on whether the output level of the SR system y_i is positive or negative. Comparator and Schmitt trigger differ in one respect only; the current output sample of the Schmitt trigger $y_i[n]$ depends on the previous sample $y_i[n-1]$. Thus, the BER is derived from the Markov model shown in Fig. 5.

As an example, consider the case of $N = 2$ and $d_i = +1$. Errors occur when the sample $y_i[0] = -V$ and $y_i[1] = +V$, $y_i[0] = -V$ and $y_i[1] = -V$, and $y_i[0] = +V$ and $y_i[1] = +V$; probabilities of these errors are denoted $P_{+V\to-V} \times P_{-V\to+V}$, $P_{+V\to-V} \times P_{-V\to-V}$, and $P_{+V\to+V} \times P_{+V\to+V}$, respectively. In the case of $N = 2$ and $d_i = -1$, errors occur when $y_i[0] = +V$ and $y_i[1] = -V$, with probabilities of $P_{+V\to+V} \times P_{+V\to-V}$. Thus, in the case of $N = 2$, the BER is derived as follows.

$$\begin{aligned}
&\mathrm{BER}(N=2)\\
&= \frac{1}{2}\mathrm{erfc}\left(\frac{\eta + A}{\sqrt{2(\sigma_c^2 + \sigma_{SR}^2)}}\right) \times \frac{1}{2}\mathrm{erfc}\left(\frac{\eta + A}{\sqrt{2(\sigma_c^2 + \sigma_{SR}^2)}}\right)\\
&\quad + \frac{1}{2}\mathrm{erfc}\left(\frac{\eta + A}{\sqrt{2(\sigma_c^2 + \sigma_{SR}^2)}}\right) \times \left\{1 - \frac{1}{2}\mathrm{erfc}\left(\frac{\eta + A}{\sqrt{2(\sigma_c^2 + \sigma_{SR}^2)}}\right)\right\}\\
&\quad + \left\{1 - \frac{1}{2}\mathrm{erfc}\left(\frac{\eta + A}{\sqrt{2(\sigma_c^2 + \sigma_{SR}^2)}}\right)\right\} \times \left\{1 - \frac{1}{2}\mathrm{erfc}\left(\frac{\eta - A}{\sqrt{2(\sigma_c^2 + \sigma_{SR}^2)}}\right)\right\}\\
&\quad + \left\{1 - \frac{1}{2}\mathrm{erfc}\left(\frac{\eta - A}{\sqrt{2(\sigma_c^2 + \sigma_{SR}^2)}}\right)\right\} \times \frac{1}{2}\mathrm{erfc}\left(\frac{\eta + A}{\sqrt{2(\sigma_c^2 + \sigma_{SR}^2)}}\right).
\end{aligned} \tag{17}$$

The BER for $N > 2$ is derived in the same manner.

4. Numerical results

In this section, we evaluate the BER performance installed with the Schmitt trigger, comparator, and three-level device. We show that our proposed three-level device outperforms the Schmitt trigger and comparator. First, we present analytical and numerical simulation results of the Schmitt trigger and comparator. The results show that the performance of the comparator is superior to that of the Schmitt trigger. Next, we compare the exact BER of the three-level device with that of the Schmitt trigger and comparator in Sec. 4.2 and Sec. 4.3, respectively. Numerical results show that the three-level device exhibits the best performance among these devices.

4.1 BER performances of SR receivers installed with Schmitt trigger and a comparator

Figure 6 plots the BER performance versus the PSD of the intentional noise in SR receivers installed with the Schmitt trigger and the comparator. Solid lines and points represent analytical and sim-

Table I. Parameter settings in computer simulation.

Parameter	Value
Channel noise and intentional noise	AWGN
PSD of Channel noise [10^{-21} W/Hz]	4.1
Symbol duration T_s [μs]	1.0
Received signal level A [μV]	1.0
Sensitivity of conventional receiver η [μV]	1.1
Numbers of samples per symbol N	10
Number of trials for simulation	10^5

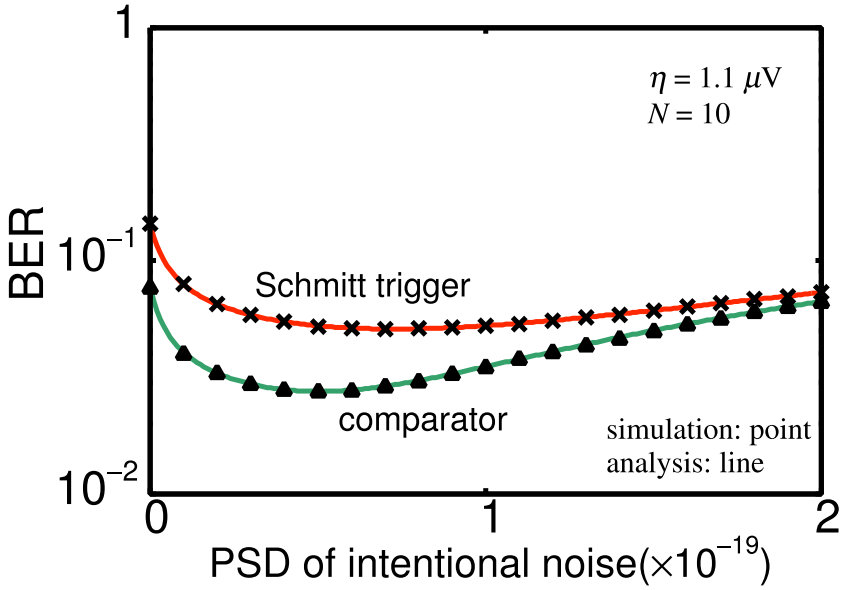

Fig. 6. BER performances of Schmitt trigger- and comparator-based SR receivers.

ulation results, respectively. Parameter settings are shown in Table I. Clearly, BER performances improve with increasing PSD of the intentional noise. This trend typifies the SR phenomenon. The figure also reveals the applicability of the analysis method to the system model because analytical and simulation results perfectly coincide.

Unexpectedly, the minimum BER of the comparator is lower than that of the Schmitt trigger. Given the memory effect of the Schmitt trigger, its performance should outshine that of the comparator.

For further discussion, we consider the dominant error in the SR receiver with the comparator. In Eq. (12), we assume that the term $\frac{1}{2}\mathrm{erfc}(\frac{\eta+A}{\sqrt{2(\sigma_c^2+\sigma_{SR}^2)}}) \sim 0$ because the function $\mathrm{erfc}(u)$ is monotonically decreasing and approaches zero at sufficiently large u. Under this assumption, all terms other than at $x = N/2$ (and $y = 0$) are neglected. Eq. (12) reduces to the equation as follows:

$$\mathrm{BER} \sim \left\{1 - \frac{1}{2}\mathrm{erfc}\left(\frac{\eta - A}{\sqrt{2(\sigma_c^2 + \sigma_{SR}^2)}}\right)\right\}^{N/2}. \tag{18}$$

BERs computed by Eq. (18) for different sample numbers per symbol ($N = 6$ and 10) are plotted as dashed lines in Fig. 7 (the solid lines plot the BER performance of the SR receiver with the comparator). Other parameter settings are unchanged from the previous analysis. Clearly, results of Eq. (18) almost match the BER performance in the relatively small PSD of the intentional noise. Thus, the non-neglected term of Eq. (18) dominates the error. In a large PSD of intentional noise, there is a gap between the solid line and dashed line. This occurs because the large PSD of intentional noise means a small argument u of $\mathrm{erfc}(u)$. Thus, the effect of the neglected term on BER performance increases.

Equation (18) computes the probability that at a received signal level A ($< \eta$), $N/2$ samples have not exceeded the threshold η of the comparator. This probability governs the BER performance of

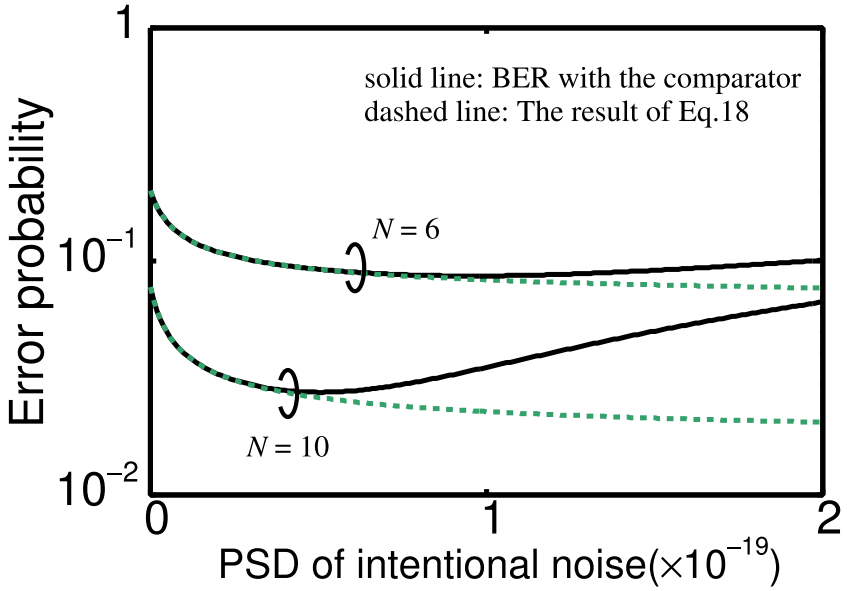

Fig. 7. Dominant errors in BER performances of the comparator-based SR receiver.

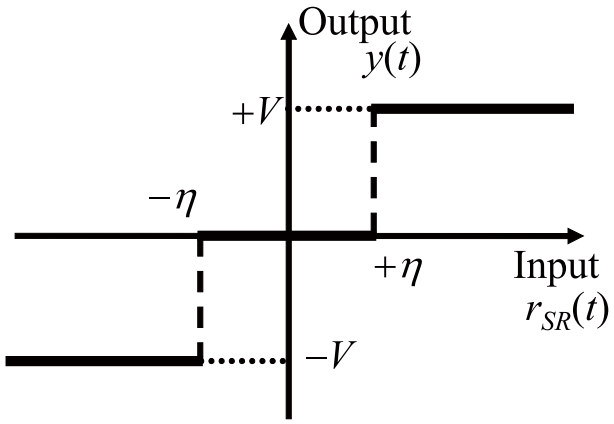

Fig. 8. Input-output characteristics of the three-level device.

the comparator-based system, and the error probability is decreased by increasing intentional noise. However, the dominant error in the Schmitt trigger is not easily decided because it also depends on the memory of the Schmitt trigger. To answer the question "Why does the comparator outperform the Schmitt trigger?," we compare performances of SR receivers installed with the Schmitt trigger and three-level device.

4.2 Performance comparison of SR receivers installed with a Schmitt trigger and three-level device

In this subsection, we discuss why a Schmitt trigger yields a poorer BER performance than a non-dynamical device in an SR receiver. We surmise that the memory feature of a Schmitt trigger negatively affects BER performance. To explain this effect, we consider the three-level device, a simple threshold device without a memory (see Fig. 8). Similar to a Schmitt trigger, the three-level device has two non-zero outputs and two thresholds but admits an additional zero output with no contribution to detection.

In our previous research, we proposed an analysis method for the SR receiver installed with the three-level device [10]. Using the same method, we now compare performances of these devices. Figure 9 plots the BER performance versus the PSD of the intentional noise in SR receivers installed with the Schmitt trigger and three-level device. Parameter settings are those of Table I. The three-level device outperforms the Schmitt trigger, because of its zero output in the subthreshold region

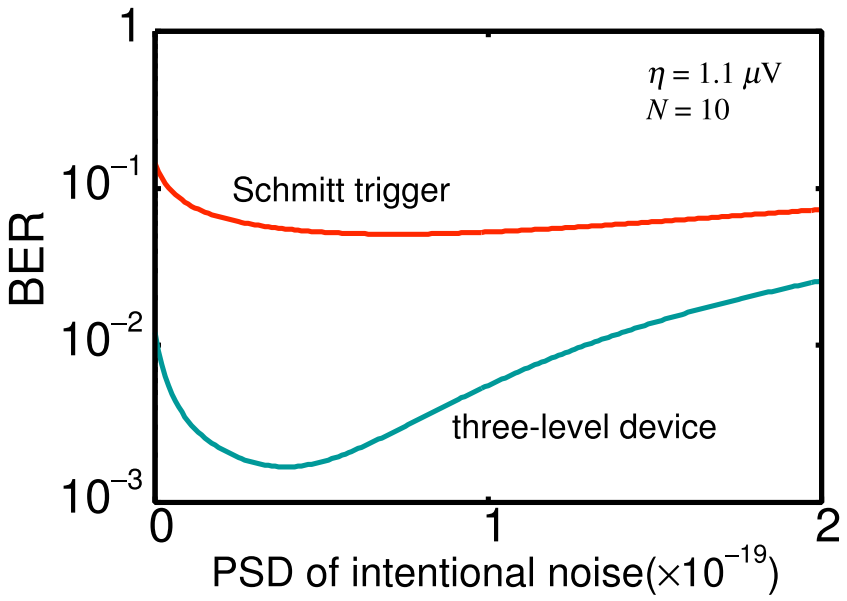

Fig. 9. BER performance of the SR receiver based on the three-level device.

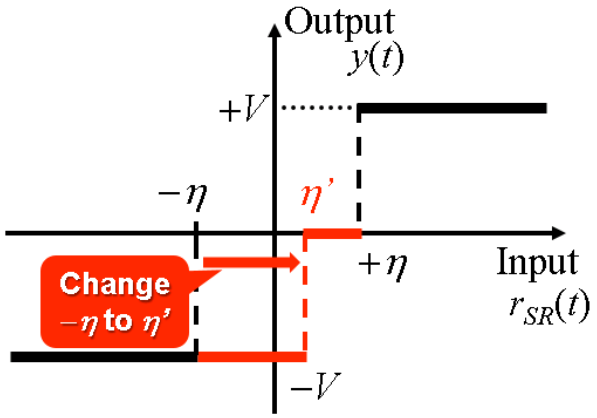

Fig. 10. Input-output characteristics of three-level device after changing the threshold.

which cannot be detected by conventional receivers. In the Schmitt trigger, information is maintained in the subthreshold region, degrading the BER performance. Moreover, unlike the comparator, the three-level device is strongly compatible with binary communication systems. Performances of the comparator and three-level device are compared in the next subsection.

4.3 Performance comparison of SR receivers installed with comparator and three-level device

This subsection compares performances between the comparator and three-level device. For this purpose, we change the threshold $-\eta$ to η' within the subthreshold region $\eta' \leq -A$ or $A \leq \eta'$, as shown in Fig. 10. According to characteristics, the output of the three-level device alters as follows:

$$y(t) = \begin{cases} +V & (r_{\mathrm{SR}}(t) > \eta) \\ -V & (r_{\mathrm{SR}}(t) < \eta') \\ 0 & otherwise \end{cases}. \tag{19}$$

When $\eta' = \eta$, input-output characteristics of the three-level device and comparator coincide.

Figure 11 plots BER performances of the three-level device after changing the threshold. Specifically, we increased the threshold η' from $1.0\mu V$ to $1.1\mu V$, maintaining other parameters at their values in Table I. In this situation, the received signal level is below the device threshold. As the threshold

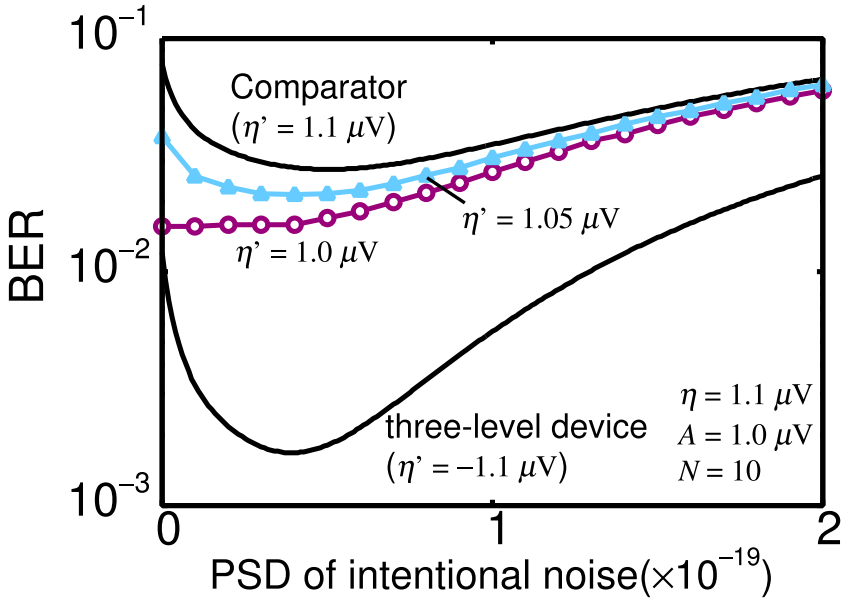

Fig. 11. BER performances of three-level device after changing the threshold.

η' approaches η, BER performances of the three-level device and comparator converge. This analysis demonstrates the superior BER performance of the three-level device over the comparator.

5. Conclusion

In this study, we considered a binary communication with SR systems for subthreshold signal reception. We focused on the basic SR devices of the Schmitt trigger, comparator, and three-level device and compared the performance of these devices. For comparison of these devices, we proposed an analysis method for SR receivers installed with a Schmitt trigger and a comparator and evaluated BER performances of both devices. Numerical results show improvements of the BER performances by SR and exactly coincide with calculated BER performances. In performance comparisons, the comparator was found to outperform the Schmitt trigger. The poorer performance of the Schmitt Trigger was attributed to the memory effect, which degrades subthreshold signal reception. We then compared the BER performance of our three-level device (a simple threshold device without a memory) with those of comparator and Schmitt trigger. According to numerical results, our three-level device exhibits the strongest performance among the tested devices; moreover, it is compatible with binary communication systems.

Acknowledgments

The authors would like to note that discussions with Prof. Masaaki Katayama, associate Prof. Hiraku Okada and assistant Prof. Kentaro Kobayashi have been illuminating this study. A part of this work is supported by KAKENHI, Grant-in-Aid for Scientific Research 26630174, and THE HORI SCIENCES AND ARTS FOUNDATION.

References

[1] F. Chapeau-Blondeau and D. Rousseau, "Noise-enhanced performance for an optimal bayesian estimator," *IEEE Transactions on Signal Processing*, vol. 52, no. 5, pp. 1327–1334, May 2004.

[2] S. Kay, "Can detectability be improved by adding noise?" *IEEE Signal Processing Letters*, vol. 7, no. 1, pp. 8–10, January 2000.

[3] A. Patel and B. Kosko, "Optimal noise benefits in neyman-pearson and inequality-constrained statistical signal detection," *IEEE Transactions on Signal Processing*, vol. 57, no. 5, pp. 1655–1669, May 2009.

[4] D.V. Dylov and J.W. Fleischer, "Nonlinear self-filtering of noisy images via dynamical stochastic resonance," *Nat Photon*, vol. 4, no. 5, pp. 323–328, May 2010. [Online]. Available: http://dx.doi.org/10.1038/nphoton.2010.31

[5] Z. Gingl, L.B. Kiss, and F. Moss, "Non-dynamical stochastic resonance: Theory and experiments with white and arbitrarily coloured noise," *EPL (Europhysics Letters)*, vol. 29, no. 3, p. 191, 1995. [Online]. Available: http://stacks.iop.org/0295-5075/29/i=3/a=001

[6] A. Ichiki and Y. Tadokoro, "Relation between optimal nonlinearity and non-gaussian noise: Enhancing a weak signal in a nonlinear system," *Phys. Rev. E*, vol. 87, p. 012124, January 2013. [Online]. Available: http://link.aps.org/doi/10.1103/PhysRevE.87.012124

[7] H. Ham, T. Matsuoka, and K. Taniguchi, "Application of noise-enhanced detection of subthreshold signals for communication systems," *IEICE Trans. Fundamentals*, vol. E92-A, no. 4, pp. 1012–1018, April 2009.

[8] S. Sugiura, A. Ichiki, and Y. Tadokoro, "Stochastic-resonance based iterative detection for serially-concatenated turbo codes," *IEEE Signal Processing Letters*, vol. 19, no. 10, pp. 655–658, October 2012.

[9] D. He, Y. Lin, C. He, and L. Jiang, "A novel spectrum-sensing technique in cognitive radio based on stochastic resonance," *IEEE Transactions on Vehicular Technology*, vol. 59, no. 4, pp. 1680–1688, May 2010.

[10] H. Tanaka, K. Chiga, T. Yamazato, Y. Tadokoro, and S. Arai, "Noise-enhanced subthreshold signal reception by a stochastic resonance receiver using a non-dynamical device," *IEICE Nonlinear Theory and Its Applications*, vol. 6, no. 2, pp. 303–312, 2015.

[11] K. Chiga, H. Tanaka, T. Yamazato, Y. Tadokoro, and S. Arai, "Development of add-on stochastic resonance device for the detection of subthreshold rf signals," *to be appeared in Nonlinear Theory and Its Applications, IEICE*, 2015.

[12] B. McNamara and K. Wiesenfeld, "Theory of stochastic resonance," *Phys. Rev. A*, vol. 39, pp. 4854–4869, May 1989. [Online]. Available: http://link.aps.org/doi/10.1103/PhysRevA.39.4854

[13] V.I. Melnikov, "Schmitt trigger: A solvable model of stochastic resonance," *Phys. Rev. E*, vol. 48, pp. 2481–2489, October 1993. [Online]. Available: http://link.aps.org/doi/10.1103/PhysRevE.48.2481

[14] A. Ichiki, Y. Tadokoro, and M. Takanashi, "Sampling frequency analysis for efficient stochastic resonance in digital signal processing," *J. Sig. Process*, vol. 16, no. 6, pp. 467–475, November 2012.